Probabilistic Assessment of Biodeterioration Effects on Reinforced Concrete Sewers

Jorge Fernando Marquez-Peñaranda, Mauricio Sanchez-Silva, Emilio Bastidas-Arteaga

corrosion and materials degradation

MDPI

Article

Probabilistic Assessment of Biodeterioration Effects on Reinforced Concrete Sewers

Jorge Fernando Marquez-Peñaranda [1], Mauricio Sanchez-Silva [2] and Emilio Bastidas-Arteaga [3,*]

[1] Departamento de Construcciones Civiles, Universidad Francisco de Paula Santander, Avenida Gran Colombia No. 12E-96 Colsag, Cucuta 540003, Colombia; jorgefernandomp@ufps.edu.co
[2] Department of Civil and Environmental Engineering, Universidad de Los Andes, Carrera 1 Este No. 19A-40, Edificio Mario Laserna, Piso 6, Bogota 111711, Colombia; msanchez@uniandes.edu.co
[3] Laboratory of Engineering Sciences for the Environment (LaSIE UMR CNRS 7356), La Rochelle Université, Avenue Michel Crépeau, CEDEX 1, 17042 La Rochelle, France
* Correspondence: ebastida@univ-lr.fr; Tel.: +33-(0)5-86-56-22-32

Abstract: The worldwide current practice of the structural design of sewers is based on procedures which usually include the effects caused by chemical and biological deterioration. However, in the last few decades, many sewer pipes have been designed using reinforced concrete which have succinctly considered such deterioration promoters. Indeed, knowledge related to reinforced concrete deterioration processes has become an important issue when forecasting the expected or remaining lifespan of sewers. Within these processes, thickness and strength losses and porosity augments have been found to be the result of the vital activity of sulfur-oxidizing bacteria and some types of fungus. This paper presents a rational methodology that uses biodeterioration measurements to describe how biodeterioration effects can affect the probability of failure during the lifetime of sewers. The probability of failure was obtained using Monte Carlo simulations based on numerical sampling from lognormal and uniform distributions. The concrete and reinforcement strength, geometric properties, H_2S concentration in the headspace, and load values were considered as the main sources of uncertainty. The results indicate that the expected service lifespan can vary between 55 and 37 years for low and high H_2S concentrations, respectively.

Keywords: biodeterioration; buried sewers; bending strength; probability of failure

Citation: Marquez-Peñaranda, J.F.; Sanchez-Silva, M.; Bastidas-Arteaga, E. Probabilistic Assessment of Biodeterioration Effects on Reinforced Concrete Sewers. *Corros. Mater. Degrad.* **2022**, *3*, 333–348. https://doi.org/10.3390/cmd3030020

Academic Editors: Miguel-Ángel Climent and Carmen Andrade

Received: 12 June 2022
Accepted: 4 July 2022
Published: 10 July 2022

1. Introduction

Reinforced concrete sewers are usually exposed to highly varying and aggressive work conditions during their lifetimes. They are built underground, supporting important infill and traffic loads which can lead to soil settlement and structural material cracking [1]. Inside a typical sewer, different hazards can arise for its structure: (a) diluted and deposited solid matter and the velocity variability of running water can modify the surfaces roughness and the concrete cover thickness [2], (b) the existence of gases such as carbon dioxide and hydrogen sulfide promote chemical deterioration [3], (c) byproducts coming from the growth of microorganisms existing in wastewater and moist walls increase the harmful chemical reactions [4], (d) concrete strength losses with subsequent cross-section reduction change the structural properties [5–9], (e) the variability of the real hydrogen sulfide concentration imposes high uncertainty in deterioration processes [10–15], (f) superimposed loads and biodeterioration processes typically lead to the prevalence of pipe crown failure [16–21], and (g) chloride diffusion can corrode the steel reinforcement [22,23]. The combination of mechanical, chemical, and biogenic hazards can reduce the sewer's service life significantly [24,25].

The sewer's failure affects infrastructure investment adversely and jeopardizes human health [26]. Hence, appropriate design and management procedures are indispensable for the optimization of the sewer's level of service. However, although modern design aids

and data from powerful sewer inspection systems are available [10,11,27–29], the current design practice is still based on procedures which are mainly focused on the mechanical relationships of the problem [28,30,31]. Likewise, the inclusion of chemical and biogenic aspects has been strongly recommended. Nonetheless, most designers still emphasize their work in solving exclusively physically related algorithms [32,33].

Concrete weight, strength losses, and porosity augments are related to the early failure of sewers. Although there is evidence of 70-year-old sewers maintaining an acceptable service level, others have failed after only ten years of service [29,30,34,35]. The differences in the performance of these systems can be associated with wastewater quality variations, material behavior, and wastewater flow characteristics. Some research works have suggested that the legislation for the reduction of metal contaminants in sewer systems, promulgated in the 1980s in the USA and Europe, brought an important diminution of biologically toxic elements within sewers, allowing a larger and faster proliferation of microorganisms capable of producing biodeterioration [10,11,36,37]. In addition, the increased wastewater transport demand of the last few years has produced important augments in the caudal, velocity and turbulence of running water, which remove the layers of corroded material formed over years. The corroded layer's removal facilitates continuous biofilm renewal on exposed surfaces and the penetration of the front of biodeterioration into deeper layers of the concrete matrix [38–41].

This paper proposes a methodology to assess the reliability of sewer pipes subjected to biodeterioration effects. The mechanical strength and demand variation of the bending moment in the crown and walls of a typical sewer are forecasted. The document is organized in seven sections. Section 2 presents some topics related to the effects of biodeterioration on the material properties. Section 3 summarizes the fundamentals and procedures currently used in the structural design of sewers. Section 4 describes a proposal to incorporate the effect of biogenic activity in the structural design of sewers. In Section 5, a practical example of the proposed methodology is solved. Finally, Sections 6 and 7 state the conclusions and recommendations.

2. Influence of Biodeterioration on Concrete Properties

Biodeterioration kinematics can accelerate harmful effects on concrete such as carbonation and cracking in sewers [5,42,43]. On the other hand, the ecology of the microbial communities is highly dependent on the concrete pH [12,16]. The high alkalinity of new concrete (a pH of about 12) inhibits microbial development upon the inner surfaces. However, carbonation and exposure to hydrogen sulfide reduce the concrete pH to a point at which neutrophilic bacteria and fungi can thrive, producing acidic metabolites which in turn lower the pH to a point at which acidophilic bacteria appear [44]. The porosity increase and strength and weight losses have been associated mainly to sulfur oxidizing bacteria (SOB) and the activity of some fungi [45,46]. SOB oxidize hydrogen sulfide or reduced sulfur compounds and produce sulfate or sulfuric acid [47–49]. Sulfuric acid reacts with the calcium hydroxide of the cement matrix, forming calcium sulfate. In turn, the calcium sulfate reacts with calcium aluminate hydrate to form ettringite, which is an expansive material capable of breaking the superficial concrete layers [50–52]. *Acidithiobacillus thiooxidans*, *Halothiobacillus neapolitanus*, *Starkeya novella*, and *Thiomonas intermedia* are SOB which are widely known as promoters of concrete biodeterioration. Furthermore, the fungus *Fusarium* has been found to be capable of concrete deterioration, but the most aggressive strains are all SOB members of the phylum proteobacteria [3,12,53–57].

Concrete sewer maintenance and reparation activities related to the durability detriment due to biodeterioration effects are costly [26,58,59]. In biodeterioration processes, the durability detriment is mainly related to the development of a layer of high porosity produced by acid attack. This layer makes the concrete more permeable, less resistant, and susceptible to the greater diffusion of nocuous agents [60–64]. Three stages which are dependent on the pH of wet sewer surfaces have been proposed to describe the chronology of biodeterioration [11,54]. In the first stage, high alkalinity (pH > 9) significantly inhibits

the microbial activity, and no deterioration is observed. Nonetheless, carbonation and the presence of hydrogen sulfide cause the pH to decay continuously. In the second stage (pH ranging from 9 to 4), neutrophilic organisms are responsible for medium-to-high thickness losses. Recently, the fungus *Fusarium* was found to be capable of producing thickness losses of up to 2.3 mm/year during the first year [16,46]. In the third stage, acidophilic bacteria produce severe thickness losses and rapid acidification (pH < 4). Each stage has a high uncertainty and can take months or years to develop. For this reason, biodeterioration must be modeled as a time-variant process throughout the structural lifetime [65].

A wide range of concrete weight and thickness losses produced by SOB and other microorganisms has been reported in the literature. Table 1 presents a summary of such findings. The large variation in measurements related to biodeterioration and its effect upon the durability of reinforced concrete sewers can be explained by considering the following facts:

Table 1. Concrete losses produced by biodeterioration according to the literature.

Exposure Time (Days)	Weight Loss	Thickness Loss (mm/Year)	Environment	Experimental Conditions	Ref.
20	N.A.	3.50	1100 ppm H_2S, 21.5 °C	Pilot-scale sewer pipe	[66]
40	N.A.	10	89 ppm H_2S, 17 °C	In situ (real env.)	[13]
68	N.A.	5.37	250 ppm H_2S	Experimental apparatus	[67]
81	N.A.	2.59	N.A.	Experimental apparatus	[68]
120	1.6%	0.16 [a]	100–200 ppm H_2S, 25–30 °C	In situ (real env.)	[14]
180	N.A.	20	700–1000 ppm H_2S, 20–35 °C	Pilot scale system	[17]
227	N.A.	0.21	300–600 ppm H_2S, 23 °C	Reactor in laboratory	[69]
270	5.8%	0.20 [a]	12–18 ppm H_2S	Simulation chamber	[53]
300	6.8%	0.30 [a]	8–15 ppm H_2S, 30 °C	Experimental apparatus	[6]
350	100%	20	5–15 ppm H_2S, 30 °C	Simulation chamber	[70]
360	37.0%	10	10–50 ppm H_2S	In situ (real env.)	[12]
930	N.A.	12	79 ppm H_2S	In situ (real env.)	[11]
960	N.A.	8.9	50 ppm H_2S, 30 °C	Corrosion Chamber	[27]
1350	N.A.	1.0	5–50 ppm H_2S,	Corrosion Chamber	[18]
1460	N.A.	1.0	5 ppm H_2S, 21 °C	In situ (real env.)	[10]
1460	N.A.	0.5	68 ppm H_2S, 27 °C	In situ (real env.)	[10]
1460	N.A.	0.1	650 ppm H_2S, 27 °C	In situ (real env.)	[10]
1620	N.A.	0.19	5–50 ppm H_2S, 25 °C	Corrosion Chamber	[19]

[a] Thickness loss computed from data considering a uniform thickness loss around the sample.

- Biodeterioration can reduce the expected service life span from 50–100 years to less than 10 years [17].
- Biodeterioration initiation can take 0.3 to 2.2 years to occur [6,11,12,71]. This lapse has been associated with the environmental conditioning needed for living organisms' adaptation.
- Temperature and relative humidity variations in the headspace can modify the sulfide uptake and lead to important variations in biodeterioration dynamics [27].
- Real H_2S concentrations can vary from a few to hundreds of ppm. It has been observed that concrete deterioration increases when the H_2S concentration becomes higher [66]. The biological and chemical nature of deterioration processes impose high variability in the sewer behavior, such that the use of analysis with probabilistic models is highly recommended [6,18,27,71].
- Old concrete surfaces tend to deteriorate more rapidly than new ones. In similar environmental conditions, old concrete surfaces can deteriorate seven to 80 times faster than new ones [10,19].
- Biodeterioration effects are typically concentrated in zones located in crown and waterline walls. The washing effect produced by running water and temperature and relative humidity variations lead to larger thickness losses in the waterline walls than

in the crown. Thickness losses in the waterline walls can vary from two to four times those in the crown [16–19].

- The bending capacity of reinforced concrete is reduced rapidly because of rebar steel corrosion produced by hydrogen sulfide attack. Steel thickness losses of 0.30 to 85 mm/year have been reported for environments containing up to 850 ppm H_2S [17,71–74].
- Rapid concrete strength losses produce cross-section reduction due to the drop off or remotion of superficial deteriorated concrete layers [5–9]

The facts previously exposed and the data from Table 1 were used to compute the numerical ranges of some of the variables described in Section 5.

3. Current Practice in the Structural Design of Sewers

Most reinforced concrete sewer facilities are built underground. Hydraulic demands, the structural stiffness of the conduits, the surrounding infill, soil heterogeneity, seismic events and overlaid traffic are important aspects to consider when designing a sewer pipe [32]. A typical structural design approach considers the following: (a) hydraulic design is an input; (b) short-duration overpressure or vacuum loading are not generated; (c) soil–structure interaction analysis is used to infer how the pipes and surrounding soil move together [1,75,76]; (d) lateral earth loads, soil reactions, friction loads and settlements and other displacements can be obtained from static analysis; (e) gravity loads from traffic, soil fill weight, the weight of the pipe, and wastewater weight are static actions applied in varying locations and forms [77]; (f) reinforced concrete lines show low vulnerability to seismic demands because they are built connecting short rigid spans of pipe by means of unrestrained joints; (g) for partially or totally buried pipes, the low probability of the coincidence of seismic loads and larger values of gravity or lateral earth loads allow us to obviate the seismic considerations in the structural design [78–80].

Some particularities used in the load analysis within the current practice for the structural design of reinforced concrete sewers can be summarized as follows:

- Pipes are placed underground following two configurations: trench and positive embankment. In the trench case, due to the backfill settlement, friction forces at the backfill–in situ material interface will reduce the gravity effects upon the pipe. In the embankment case, the soil placed on the sides of the pipe will settle more than the soil above the pipe, imposing larger gravity loads above the pipe. In both cases, gravity and lateral thrust effects are included in the structural analysis. This paper deals only with the trench condition [77,81].
- The traffic load magnitude is a function of the type of superficial cover (flexible or rigid pavements, or unsurfaced cover), the depth at which the pipe is set, the class of vehicle (trucks, aircrafts, or others) and the direction of travel (parallel or perpendicular to the pipe axis). In general, the deeper the pipe location the lower the traffic effects [77,82].
- The fluid weight will vary depending on the hydraulic problems arising from the inadequate size or gradient of pipe, infiltration (from groundwater) and inflow (from surface runoff) [20,83–86].
- Figure 1 shows the typical loads upon a buried sewer pipe. *WS* is the backfill pressure (kN/m^2), *WL* is the effective traffic load (kN/m^2), *WP* is the weight of the pipe (kN/m^2), *WF* is the fluid (water weight) pressure (kN/m^2), and *ET* and *EB* are the lateral thrust pressure at the top and bottom of the pipe, respectively (kN/m^2). There is a load-spreading configuration along a pipe that is laid parallel to the traffic direction and the so called "effective supporting length of pipe (*Le*)". The bedding angle α defines the arc length where the pipe is effectively supported. The α value and reaction pressure form depend on the bedding material properties [81].

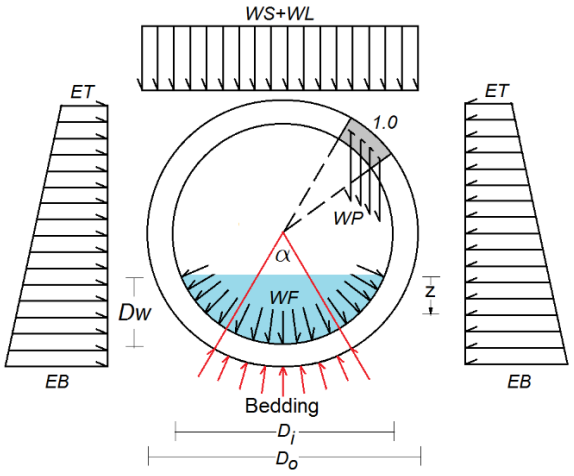

a) Cross section and typical loads in a unit length of sewer pipe

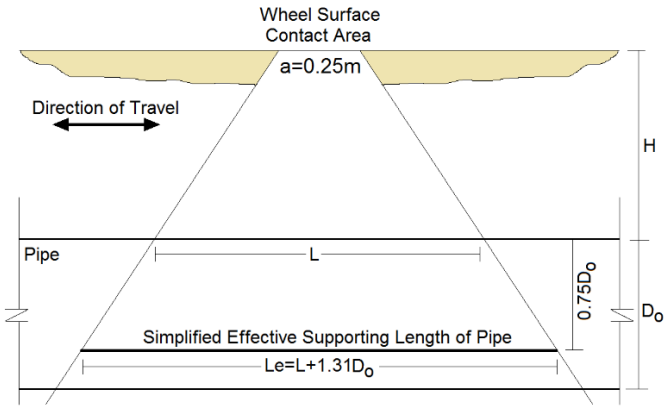

b) Typical simplified traffic load spread on a buried rigid pipe

Figure 1. Typical loads demanding a buried sewer pipe (based on information available in [81]).

The reinforced concrete pipes used as sewers typically have a low reinforcement steel ratio and thick concrete thickness which guarantee a greater shear capacity. For this reason, in this work only the bending moment capacity is considered. The bending moment capacity for singly reinforced normal-weight concrete elements can be computed using Equation (1) [87]:

$$M_n = \rho f_y \left(1 - \frac{\rho f_y}{1.7 \rho f\prime_c}\right) bd^2, \quad (1)$$

where M_n is the nominal bending capacity (KN-m), ρ is the reinforcement steel ratio, f_y is the steel yield strength (KN/m^2), $f\prime_c$ is the compressive strength of the concrete (KN/m^2), b the cross-section width (m), and d is the internal lever arm (m).

4. Structural Design of Sewers Considering Biodeterioration

Unexpected changes in the deterioration patterns make the inclusion of deterioration effects in the sewer's structural design a complex task. Factors such as age, pipe characteristics, the existence of underground water, chemical and physical soil properties, the proximity of other installations, the sewer slope, and the sewer water quality can bring a high degree of uncertainty to the processes of the analysis and design of sewers [34,84]. In order to counteract such uncertainty in the sewers' structural design practice, methods such as the addition of sacrificial thickness and the definition of allowable crack widths in the inner walls were implemented [81,88]. Furthermore, although several models using different biodeterioration rates were used, their predictions failed when compared to real

measurements. For example, some models have fitted rather well up to 20 years uptime but forecasted thickness losses of about one quarter to one third of the measured thickness changes 15 years later [34]. Indeed, thickness losses produced by biodeterioration increase the probability of failure of sewer pipes. To confront this hazard, a typical factor of safety of 1.3 is used for reinforced concrete pipes when no sacrificial layer is used [81]. Although this methodology is amicable to the designers, the uncertainty associated with the load–capacity relations demand a comprehensive methodology which considers the randomness of the process. To attend to this need, a probabilistic approach to the determination of the bending strength of a sewer is proposed and presented in this section. A summary of the approach for structural analysis is shown in Figure 2.

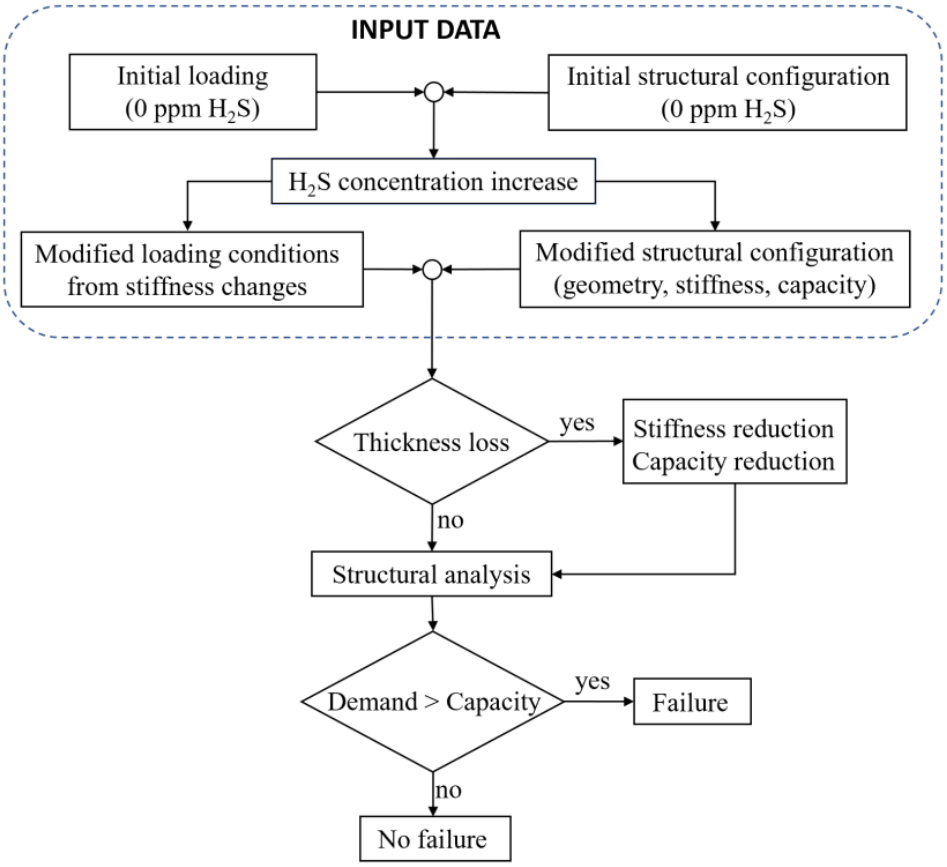

Figure 2. Flowchart of the proposed model for the structural analysis of a reinforced concrete sewer.

4.1. Structural Analysis

Typical models of sewer failure consider two critical zones in a cross section of the pipe: the crown and the waterline walls. When studying the biodeterioration effects on the structural integrity, a thickness reduction is considered in such places. In this work the direct stiffness method was used to analyze a typical sewer pipe in which the thickness at the crown and waterline walls is reduced during successive stages. Quadrangular thick plate elements are jointed to form a quasi-cylindrical duct, as shown in Figure 3. In order to compute the inner forces and nodal displacements, a MATLAB® code (R2014A, MathWorks, Natick, MA,USA) was written and then validated using the software SAP2000® (V.17.1.1, Computers and Structures Inc, Berkeley, CA) [76,89–93]. During the validation process, the lower elements of the pipe section were supported on springs to simulate the soil reactions. The spring constants were computed by multiplying the modulus of the subgrade reaction by the afferent area around the joint [75,94–96]. The structural analysis developed using the MATLAB® code was appropriate to simulate the inner forces' distribution.

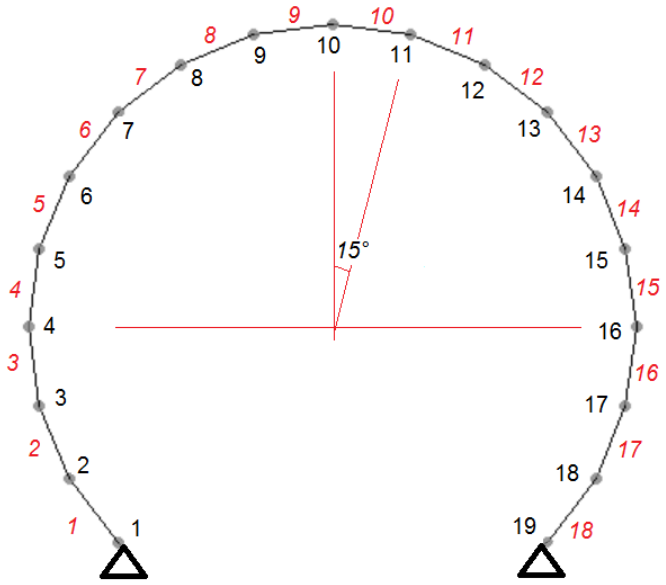

Figure 3. Model used for structural analysis in the MATLAB® code.

4.2. Probabilistic Approach

To investigate how the biodeterioration influences the structural capacity of a sewer, in this study several sources of uncertainty were considered. Lognormal or uniform probability distributions were adopted for each variable. The load mean values were calculated as indicated in Section 2, and the geometrical mean values were taken from the nominal commercial values required by the ASTM standards [97]. The resistance mean values were computed using Equations (2) and (3):

$$\mu_{Mn} = \mu_\rho \mu_{f_y} \left(1 - \frac{\mu_\rho \mu_{f_y}}{1.7 \mu_{f'_c}}\right) b {\mu_d}^2 \tag{2}$$

$$\mu_d = \left(d - \frac{t \mu_{\Delta t}}{1000}\right), \tag{3}$$

where μ_{Mn} is the mean value of the bending moment capacity (kN-m), μ_ρ is the mean value of the steel ratio (cm^2/cm^2), t is the elapsed time from the biodeterioration initiation (years), μ_d is the mean value of the reduced internal lever arm at time t (m), $\mu_{\Delta t}$ is the mean value of the thickness loss rate at time t (mm/year), μ_{f_y} is the mean value of the steel strength (kN/m^2), and $\mu_{f'_c}$ is the mean value of the concrete strength (kN/m^2).

To study how the probability of failure of the sewer pipe system behaves, a system limit state function was defined [98]:

$$g(R, S) = R - S = Z \tag{4}$$

where *g(R,S)* is the limit state function, R is the system resistance, and S is the load demand on the system. When the *g(R,S)* value is negative, system failure is expected. On the contrary, if the *g(R,S)* value is positive or zero, the system will show safe behavior. In this work, the R and S values are obtained from the vector of capacities linked to the mean values given by Equations (2) and (3) and from the vector of effects (internal bending moments) produced by the loads defined in Section 2, respectively. The probability of failure can be estimated as [98]

$$p_f = \Phi\left(-\frac{\mu_Z}{\sigma_Z}\right) = \Phi(-\beta) \tag{5}$$

where p_f is the probability of failure, $\Phi(\cdot)$ is the standard normal probability distribution with an expected value equal to 0 and a standard deviation equal to 1, μ_Z is the mean value of Z, and σ_Z is the standard deviation of Z. Crude Monte Carlo simulations were used to propagate uncertainties in the deterministic model in order to estimate the probability of failure [98–100]. Random values were first generated. They were then propagated in the mechanical model to evaluate the limit state functions. The number of fails was finally counted to estimate the probability of failure.

5. Example: Reliability Assessment of Sewers Considering Biodeterioration

5.1. Description

A reinforced concrete pipe will be placed under a road with a high traffic of trucks into a 3.60 m × 6.57 m (width × depth) trench. The pipe's inner diameter and thickness wall are 2.13 m and 0.22 m, respectively. Ordinary granular material will be used in the backfill, and a granular cradle 50 mm thick will be compacted under the pipe's invert. The reinforcement configuration is shown in Figure 4 and was determined from the results of a classic analysis (considering a factor of safety of 1.30). The geometrical requirements stated in the ASTM standards were fulfilled [97,101–103]. A triple cage was specified, but an elliptical cage must not be considered when computing the bending strength. The bending moment strength can be computed following the classical reinforced concrete design theory using the characteristics of the variables described in Table 2. To study how biodeterioration influences the structural behavior, the probability of failure of the system will be determined, taking in consideration the influence of thickness losses and steel reinforcement corrosion upon the bending capacity throughout the time.

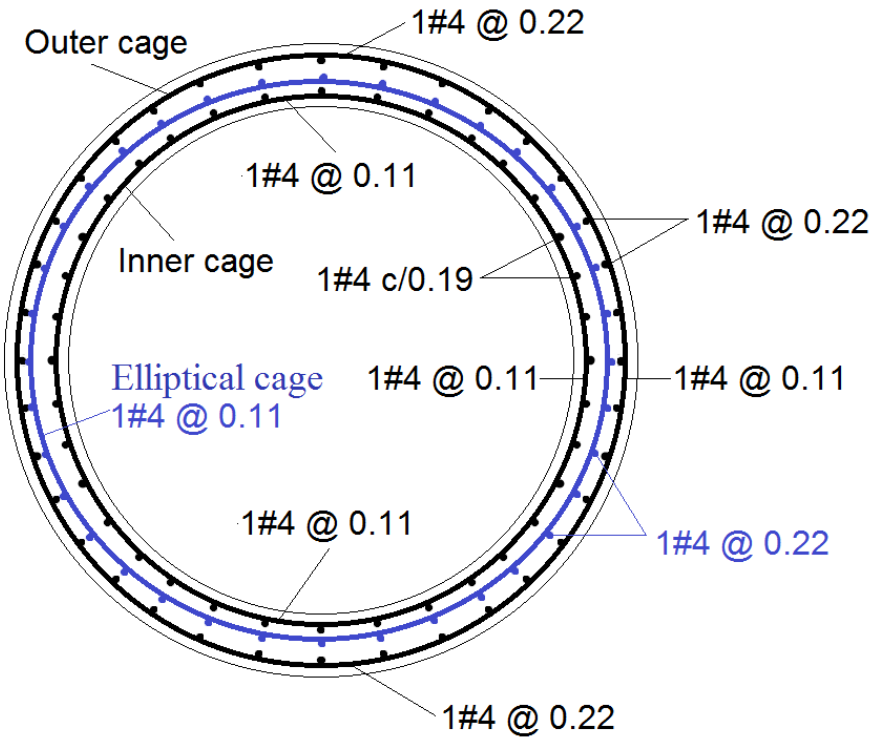

Figure 4. Steel reinforcement in a typical section. No detailing steel reinforcement is shown.

In this example, H_2S concentrations of 25, 50, 100, 200 and 400 ppm were used to include a wide range of real environments in the MATLAB® code computations. The probability of failure was calculated using Monte Carlo simulation for the crown and the waterline walls separately. The probability distribution, the mean value and coefficient of variation of the variables used in this work were obtained from the literature and are shown

in Table 2. The selection of lognormal and uniform distributions was produced based on a literature review [100,104–111]. The lognormal distributions were appropriate for parameters that cannot be physically negative, while uniform distributions were selected when the range of variation of the parameter was known.

To consider the effect of aging upon the concrete thickness loss associated to biodeterioration, a loss increment of 6.6%/year was computed from data reported in the literature [10,19]. Concrete strength losses were considered as an equivalent thickness loss, subtracting the low concrete strength thickness from the initial concrete thickness. On the other hand, the thickness loss of the steel reinforcing bars was taken as half of that calculated at any time for the concrete thickness loss at the crown. This steel/concrete loss ratio describes appropriately the remaining protection given by partially deteriorated surrounding concrete and fits well with the data reported in previous studies [24,42,71–74].

Table 2. Variables for the numerical example (references: [81,112]).

Variable	Mean Value	COV	Distribution
Concrete compressive strength, $f\prime_c$ (MPa)	28	19%	Lognormal
Reinforcement steel yield strength, f_y (MPa)	420	10%	Lognormal
Modulus of elasticity of steel, Es (MPa)	200,000	6%	Lognormal
Concrete cover to reinforcement (mm)	25	10%	Lognormal
Reinforcement steel ratio, r (cm^2/cm^2)	0.0088	5%	Lognormal
Thickness loss at the crown, Dtc (mm/year) [a]:			
H_2S concentrations up to 50 ppm	0.52	202%	Lognormal
H_2S concentration of 100 ppm	0.74	63%	Lognormal
H_2S concentration of 200 ppm	1.07	35%	Lognormal
H_2S concentration of 400 ppm	1.54	20%	Lognormal
Thickness loss ratio, Dtw/Dtc (mm/mm)	3	19%	Uniform
Biodeterioration initiation lapse (years), t_i	1.38	57%	Lognormal
Soil unit weight, γ (kN/m^3)	20	10%	Lognormal
Backfill height, H (m)	4	15%	Uniform
Traffic (live) load, P (kN) [b]	223	30%	Lognormal
Coefficient, Ku (gravel) [c]	0.165	-	Deterministic
Trench load coefficient, C [c]	0.85	-	Deterministic
Wheel load area, a × b (m × m)	0.51 × 0.25	-	Deterministic
Spread area a × b (m × m)	7.48 × 7.22	-	Deterministic

[a] A high COV suggests that biological processes (important even at low H_2S concentrations) lead to higher uncertainty that chemical processes (important at high H_2S concentrations). [b] Computed considering *WL* = P/Spread area (Section 2). [c] C and Ku are used to compute *WS*, as defined in Section 2.

5.2. Description of the Failure Modes

Current commercial reinforced concrete pipes have nominal diameters varying from 225 to 3600 mm, and typical lengths of 2440 mm. In most cases, sections of pipe are usually connected using a flexible ring capable of allowing movements in the joint. This configuration facilitates stress relief due to accommodation during a seismic event. Nevertheless, settlements could occur under the same stretch, producing stress changes within the structure. Wastewater leaks, weak bedding compaction or affectations during construction could be cited as possible causes of settlement near the ends of the pipe. However, in this work an idealized external environment where no settlements occur was considered, and two main failure modes related with concrete biodeterioration were studied: failure at the crown and failure at the waterline walls.

Figure 5 describes the sequence of thickness and bending strength loss produced by biodeterioration in sewers throughout the time. In buried sewer pipes, thickness loss from biodeterioration makes the concrete thickness decrease throughout the time (Figure 5a). The resultant smaller thickness leads to a lower inner lever arm that reduces the available bending capacity (Mn). Furthermore, it produces a lower moment of inertia that makes the bending moment (Mb) from loads change. The bending moment imposes tension stresses on the inner face of the crown and the external face of the waterline walls. Biodeterioration

attacks the inner face of the whole pipe, corroding the reinforcement steel in the crown and reducing the available compressed concrete in the waterline walls. In the crown, the tension capacity is rapidly lost due to the presence of corrosive gases which attack the reinforcement bars [62,113]. The sequence of this first failure mode (at the crown) is shown in Figure 5b. In the waterline walls, the bending capacity loss can occur more slowly because of the inner lever arm reduction. The sequence of this second failure mode (at the waterline walls) is shown in Figure 5c. In any event, there is a time t_f when the capacity can be lower than the demand and the pipe will fail. Then, a rational structural design must be used to reduce the risk and extend the lifespan of the sewer.

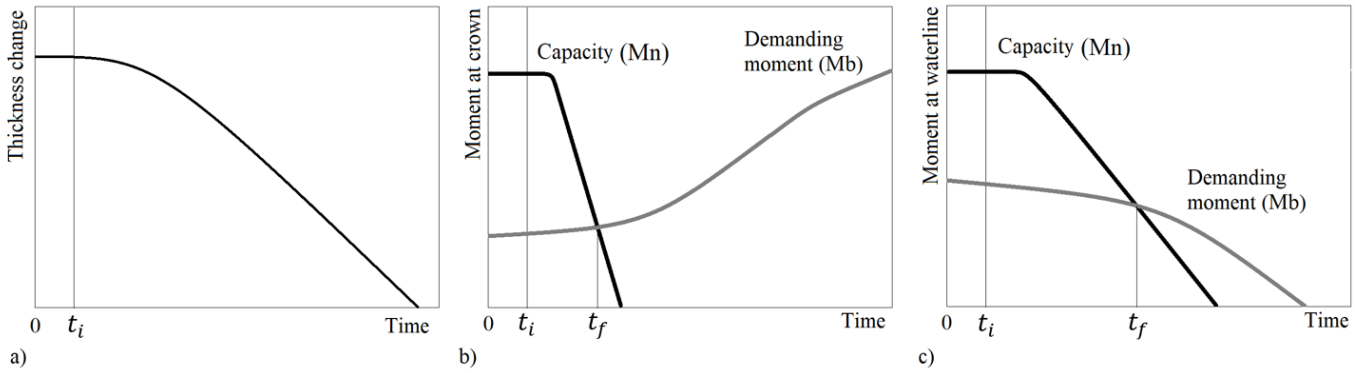

Figure 5. Sequence of changes in the thickness and strength produced by biodeterioration in sewers: (**a**) thickness change, (**b**) first failure mode produced by variations of strength and demand at the crown, (**c**) second failure mode produced by variations of strength and demand at the waterline walls.

5.3. Probability of Failure

Figure 6 shows the curves of the probability of failure obtained for the crown and the waterline walls when exposed to different H_2S concentrations. It is evident that the crown will tend to fail before than waterline walls, leading to a ceiling failure that will change the initial structural configuration drastically. In the case of crown failure (Figure 6a), the high slope of each one of the curves shows that, once the concrete cover is lost, rapid steel corrosion leads to a rapid bending strength loss. Indeed, concrete cover can significantly delay the initiation of steel corrosion. If a low probability of failure value is chosen to compute the service life of the sewer, for example p_f = 0.10, the pipe will last in service up to 55, 50, 46, 41 and 37 years when the H_2S concentration is 25, 50, 100, 200 and 400 ppm, respectively. Furthermore, the expected value (p_f = 0.50) is typically 1 to 2 years longer than the values associated to the chosen probability of failure. According to these findings, the lifespan of a sewer could reach up to 55 years if the H_2S concentration is low, and up to 37 years if the H_2S concentration is high. In the case of the waterline wall's failure (Figure 6b), for a low probability of failure (p_f = 0.10) the service life will be about 67, 61, 58, 54 and 48 years for H_2S concentrations of 25, 50, 100, 200 and 400 ppm, respectively. This means that the waterline wall's lifespan will be more than 10 years longer than that of crown.

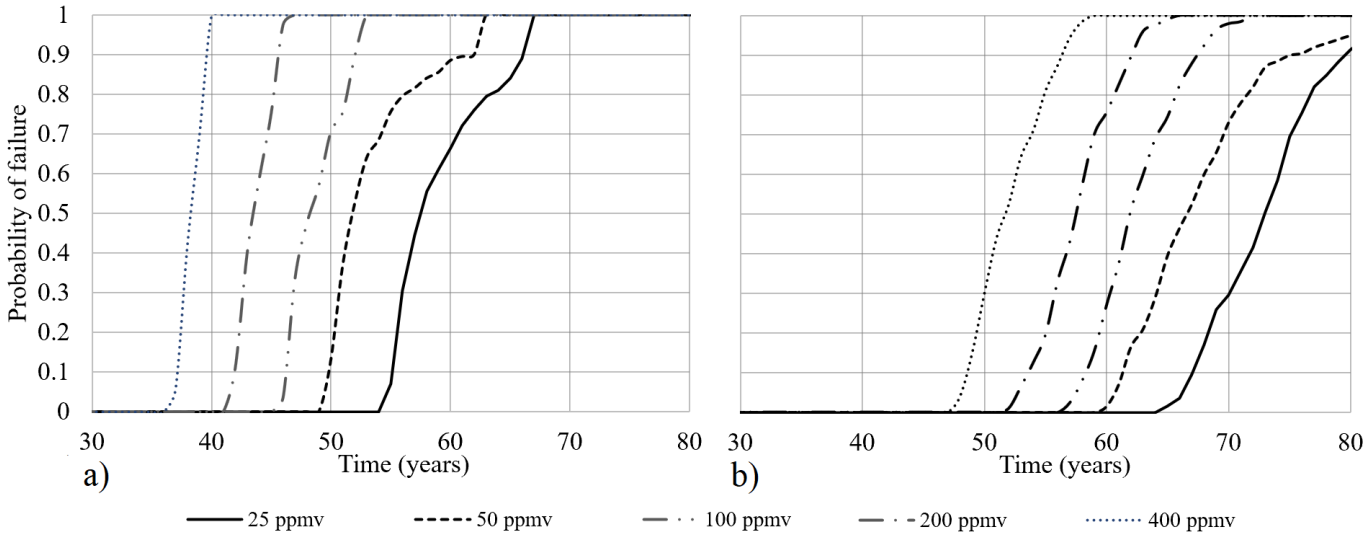

Figure 6. Probability of failure: (**a**) at the crown, and (**b**) at the waterline walls.

6. Conclusions

In this work, biodeterioration measurements, mechanical models, and stochastic simulations were used to describe how biodeterioration effects can affect the probability of failure during the lifetime of sewers. The main conclusions are summarized as follows:

- The estimated probabilities of failure show that the crown will tend to fail before than waterline walls. This finding is in accordance with the results reported in [16–21].
- A rapid bending strength loss produced by the steel corrosion at the crown or walls generates sloped curves which forecast a rapid failure once the crown concrete cover or most of the compressed concrete in the walls is lost. This conclusion coincides with real failures reported in the literature after 9 to 70 years of service [62,113].
- If the crown failure is accepted as the limit condition related to the sewer pipe failure, the expected service lifespan could be between 55 and 37 years for low and high H_2S concentrations, respectively.

7. Recommendations for Future Work

In small-diameter sewers, it is possible that the broken crown can be rearranged to develop an arch system to bear the overlaying loads upon the ceiling. More research is required to explain how this new configuration could be related to the extended life observed in deteriorated pipes.

Typical experiments using humid samples subjected to gaseous environments describe the crown environment well. However, more research is needed to understand better the existing ratio between the thickness losses in the crown and those in the waterline walls of sewers.

In sewers containing low H_2S concentrations, it is recommendable to include the effect of the inner temperature variation when modelling the biodeterioration dynamics.

Green pipes, antibacterial concrete pipes, and polyester resin concrete pipes (PRCP) are some modern options to build and partially replace sewers pipes which offer durability, wear resistance, appropriate strength, chemical resistance, and a soft inner texture. This is a wide and interesting research field to be considered in future works [114–119].

Author Contributions: Conceptualization, J.F.M.-P., M.S.-S. and E.B.-A.; methodology, J.F.M.-P., M.S.-S. and E.B.-A.; software, J.F.M.-P.; validation, J.F.M.-P., M.S.-S. and E.B.-A.; formal analysis, J.F.M.-P.; investigation, J.F.M.-P., M.S.-S. and E.B.-A.; resources, J.F.M.-P. and M.S.-S.; data curation, J.F.M.-P.; writing—original draft preparation, J.F.M.-P.; writing—review and editing, M.S.-S. and E.B.-A.; visualization, J.F.M.-P.; supervision, M.S.-S. and E.B.-A.; funding acquisition, J.F.M.-P. and M.S.-S. All authors have read and agreed to the published version of the manuscript.

Funding: This research was funded by Universidad Francisco de Paula Santander, Universidad de los Andes and COLCIENCIAS.

Institutional Review Board Statement: Not applicable.

Informed Consent Statement: Not applicable.

Data Availability Statement: The data that support the findings of this study are available upon reasonable request.

Conflicts of Interest: The authors declare no conflict of interest.

References

1. ACPA. Loads and Supporting Strengths. In *Concrete Pipe Design Manual*; American Concrete Pipe Association: Irving, TX, USA, 2011; pp. 27–82.
2. He, X.; de los Reyes, F.L.; Leming, M.L.; Dean, L.O.; Lappi, S.E.; Ducoste, J.J. Mechanisms of Fat, Oil and Grease (FOG) Deposit Formation in Sewer Lines. *Water Res.* **2013**, *47*, 4451–4459. [CrossRef] [PubMed]
3. Wei, S.; Sanchez, M.; Trejo, D.; Gillis, C. Microbial Mediated Deterioration of Reinforced Concrete Structures. *Int. Biodeterior. Biodegrad.* **2010**, *64*, 748–754. [CrossRef]
4. Jensen, H.S.; Nielsen, H.; Lens, P.N.L.; Hvitved-Jacobsen, T.; Vollertsen, J. Hydrogen Sulphide Removal from Corroding Concrete: Comparison between Surface Removal Rates and Biomass Activity. *Environ. Technol.* **2009**, *30*, 1291–1296. [CrossRef] [PubMed]
5. Bastidas-Arteaga, E.; Sánchez-Silva, M.; Chateauneuf, A.; Silva, M.R.; Ribas Silva, M. Coupled Reliability Model of Biodeterioration, Chloride Ingress and Cracking for Reinforced Concrete Structures. *Struct. Saf.* **2008**, *30*, 110–129. [CrossRef]
6. Marquez-Peñaranda, J.; Sanchez-Silva, M.; Husserl, J.; Bastidas-Arteaga, E. Effects of Biodeterioration on the Mechanical Properties of Concrete. *Mater. Struct.* **2015**, *49*, 4085–4099. [CrossRef]
7. Minch, M.Y.; Wróblewski, R.; Kmita, A. Assessment of reinforced concrete sewer after long service: A case study. *Urban Water J.* **2018**, *15*, 501–505. [CrossRef]
8. Zhang, R.; Ma, L.; Liu, P.; Chen, H.; Zhu, H.X.; Xiao, H.; Xiong, Z. Influence mechanisms under different immersion methods and different strengths of concrete in corrosive environments, and verification via long-term field test. *Struct. Concr.* **2020**, *21*, 1853–1864. [CrossRef]
9. Tscheikner-Gratl, F.; Caradot, N.; Cherqui, F.; Leitão, J.P.; Ahmadi, M.; Langeveld, J.G.; Gat, L.; Scholten, L.; Rodríguez, J.P. Sewer asset management—State of the art and research needs. *Urban Water J.* **2020**, *16*, 662–675. [CrossRef]
10. Wells, T.; Melchers, R.E. Microbial Corrosion of Sewer Pipe in Australia—Initial Field Results. In Proceedings of the 18th Intrenational Corrosion Congress, Perth, Australia, 20–24 November 2011; pp. 1–12.
11. Wells, T.; Melchers, R.E. An Observation-Based Model for Corrosion of Concrete Sewers under Aggressive Conditions. *Cem. Concr. Res.* **2014**, *61–62*, 1–10. [CrossRef]
12. Okabe, S.; Odagiri, M.; Ito, T.; Satoh, H. Succession of Sulfur-Oxidizing Bacteria in the Microbial Community on Corroding Concrete in Sewer Systems. *Appl. Environ. Microbiol.* **2007**, *73*, 971–980. [CrossRef]
13. Grengg, C.; Mittermayr, F.; Baldermann, A.; Böttcher, M.E.; Leis, A.; Koraimann, G.; Grunert, P.; Dietzel, M. Microbiologically Induced Concrete Corrosion: A Case Study from a Combined Sewer Network. *Cem. Concr. Res.* **2015**, *77*, 16–25. [CrossRef]
14. Herisson, J.; van Hullebusch, E.D.; Moletta-Denat, M.; Taquet, P.; Chaussadent, T. Toward an Accelerated Biodeterioration Test to Understand the Behavior of Portland and Calcium Aluminate Cementitious Materials in Sewer Networks. *Int. Biodeterior. Biodegrad.* **2013**, *84*, 236–243. [CrossRef]
15. Oviedo, E.R.; Johnson, D.; Shipley, H. Evaluation of hydrogen sulphide concentration and control in a sewer system. *Environ. Technol.* **2012**, *33*, 1207–1215. [CrossRef] [PubMed]
16. Hudon, E.; Mirza, S.; Frigon, D. Biodeterioration of Concrete Sewer Pipes: State of the Art and Research Needs. *J. Pipeline Syst.* **2011**, *2*, 42–52. [CrossRef]
17. Song, Y.; Tian, Y.; Li, X.; Wei, J.; Zhang, H.; Bond, P.L.; Yuan, Z.; Jiang, G. Distinct Microbially Induced Concrete Corrosion at the Tidal Region of Reinforced Concrete Sewers. *Water Res.* **2019**, *150*, 392–402. [CrossRef]
18. Jiang, G.; Keller, J.; Bond, P.L. Determining the Long-Term Effects of H_2S Concentration, Relative Humidity and Air Temperature on Concrete Sewer Corrosion. *Water Res.* **2014**, *65*, 157–169. [CrossRef]
19. Sun, X.; Jiang, G.; Chiu, T.H.; Zhou, M.; Keller, J.; Bond, P.L. Effects of Surface Washing on the Mitigation of Concrete Corrosion under Sewer Conditions. *Cem. Concr. Compos.* **2016**, *68*, 88–95. [CrossRef]

20. Salmi, E.F.; Asadi, Z.S.; Bayati, M.; Sharifzadeh, M. Assessing the Hydrogeological Conditions Leading to the Corrosion and Deterioration of Pre-cast Segmental Concrete Linings (Case of Zagros Tunnel). *Geotech. Geol. Eng.* **2019**, *37*, 3961–3983. [CrossRef]
21. Kuliczkowska, E.; Parka, A. The structural integrity of corroded concrete sewers. *Eng. Fail. Anal.* **2019**, *104*, 409–421. [CrossRef]
22. Moradian, M.; Shekarchi, M.; Pargar, F.; Bonakdar, A.; Valipour, M. Deterioration of Concrete Caused by Complex Attack in Sewage Treatment Plant Environment. *J. Perform. Constr. Facil.* **2012**, *26*, 124–134. [CrossRef]
23. Zacchei, E.; Bastidas-Arteaga, E. Multifactorial Chloride Ingress Model for Reinforced Concrete Structures Subjected to Unsaturated Conditions. *Build.* **2022**, *12*, 107. [CrossRef]
24. Imounga, H.M.; Bastidas-Arteaga, E.; Moutou Pitti, R.; Ekomy Ango, S.; Wang, X.-H. Bayesian Assessment of the Effects of Cyclic Loads on the Chloride Ingress Process into Reinforced Concrete. *App. Sci.* **2020**, *10*, 2040. [CrossRef]
25. Li, B.; Cai, L.; Zhu, W. Predicting Service Life of Concrete Structure Exposed to Sulfuric Acid Environment by Grey System Theory. *Int. J. Civ. Eng.* **2018**, *16*, 1017–1027. [CrossRef]
26. Sanchez-Silva, M.; Klutke, G.-A.; Rosowsky, D.V. Life-Cycle Performance of Structures Subject to Multiple Deterioration Mechanisms. *Struct. Saf.* **2011**, *33*, 206–217. [CrossRef]
27. Sun, X.; Jiang, G.; Bond, P.L.; Wells, T.; Keller, J. A Rapid, Non-Destructive Methodology to Monitor Activity of Sulfide-Induced Corrosion of Concrete Based on H 2 S Uptake Rate. *Water Res.* **2014**, *59*, 229–238. [CrossRef] [PubMed]
28. Erdogmus, E.; Skourup, B.N.; Tadros, M. Recommendations for Design of Reinforced Concrete Pipe. *J. Pipeline Syst. Eng. Pract.* **2010**, *1*, 25–32. [CrossRef]
29. Garcia, C.; Abraham, D.M.; Gokhale, S.; Iseley, T. Rehabilitation Alternatives for Concrete and Brick Sewers. *Pract. Period. Struct. Des. Constr.* **2002**, *7*, 164–173. [CrossRef]
30. Ejaz, N.; Hussain, J.; Ghani, U.; Shabir, F.; Naeem, U.A.; Shahmim, M.A.; Tahir, M.F. Performance of Concrete under Aggressive Wastewater Environment Using Differente Binders. *Life Sci. J.* **2013**, *10*, 141–150.
31. Erdogmus, E.; Maher, K.T. *Behavior and Design of Buried Concrete Pipes*; University of Nebraska: Lincoln, NE, USA, 2006.
32. CMA. *Design Manual for Concrete Pipe Outfall Sewers*; CMA: Bartlett Boksburg, UK, 2009; Volume 47.
33. Chughtai, F.; Zayed, T. Structural Condition Models for Sewer Pipeline. In Proceedings of the Pipelines 2007: Advances and Experiences with Trenchless Pipeline Projects, ASCE, Boston, MA, USA, 8–11 July 2007; pp. 1–11.
34. Hong, S. *Selective Inhibition of Acidophilic Thiobacilli for Application of Controlling Microbially-Induced Corrosion in Concrete Sewers*; The University of Arizona: Tucson, AZ, USA, 1992.
35. Matthews, J.C. Large-Diameter Sewer Rehabilitation Using a Fiber-Reinforced Cured-in-Place Pipe. *Pract. Period. Struct. Des. Constr.* **2014**, *04014031*, 1–5. [CrossRef]
36. Gu, J.; Mitchell, R. Biodeterioration. In *The Prokaryotes—Applied Bacteriology and Biotecnhnology*; Rosenberg, E., DeLong, E.F., Lory, S., Stackebrandt, E., Thompson, F., Eds.; Springer: Berlin/Heidelberg, Germany, 2013; pp. 309–341. ISBN 9783642313301.
37. Shifrin, N.S. Pollution Management in the Twentieth Century. *J. Environ. Eng.-ASCE* **2005**, *131*, 676–691. [CrossRef]
38. Hewayde, E.; Nehdi, M.; Allouche, E.; Nakhla, G. Effect of Mixture Design Parameters and Wetting-Drying Cycles on Resistance of Concrete to Sulfuric Acid Attack. *J. Mater. Civ. Eng.* **2007**, *19*, 155–163. [CrossRef]
39. Parande, A.K. Deterioration of Reinforced Concrete in Sewer Environments. *Proc. Inst. Civ. Eng. Munic. Eng.* **2006**, *159*, 11–20. [CrossRef]
40. Wei, S.; Jiang, Z.; Liu, H.; Zhou, D.; Sanchez-Silva, M. Microbiologically Induced Deterioration of Concrete—A Review. *Braz. J. Microbiol.* **2013**, *1007*, 1001–1007. [CrossRef] [PubMed]
41. Augustyniak, A.; Sikora, P.; Grygorcewicz, B.; Despot, D.; Braun, B.; Rakoczy, R.; Szewzyk, U.; Barjenbruch, M.; Stephan, D. Biofilms in the gravity sewer interfaces: Making a friend from a foe. *Environ. Sci. Biotechnol.* **2021**, *20*, 795–813. [CrossRef]
42. Bastidas-Arteaga, E.; Sánchez-Silva, M.; Chateauneuf, A. Structural Reliability of RC Structures Subject to Biodeterioration, Corrosion and Concrete Cracking. In Proceedings of the 10th International Conference on Applications of Statistics and Probability in Civil Engineering, Tokyo, Japan, 31 July–3 August 2007; Kanda, J., Takada, T., Furuta, H., Eds.; Taylor & Francis: London, UK, 2007; pp. 183–190.
43. Lau, I.; Li, C.-Q.; Chen, F. Analytical and Experimental Investigation on Corrosion-Induced Concrete Cracking. *Int. J. Civ. Eng.* **2020**, *18*, 99–112. [CrossRef]
44. Bielefeldt, A.; Gutierrez-Padilla, M.G.D.; Ovtchinnikov, S.; Silverstein, J.; Hernandez, M. Bacterial Kinetics of Sulfur Oxidizing Bacteria and Their Biodeterioration Rates of Concrete Sewer Pipe Samples. *J. Environ. Eng.* **2010**, *136*, 731–738. [CrossRef]
45. Gu, J.; Ford, T.E.; Berke, N.S.; Mitchell, R. Biodeterioration of Concrete by the Fungus Fusariuml. *Int. Biodeterior. Biodegrad.* **1998**, *41*, 101–109. [CrossRef]
46. George, R.P.P.; Ramya, S.; Ramachandran, D.; Kamachi Mudali, U. Studies on Biodegradation of Normal Concrete Surfaces by *Fungus Fusarium* Sp. *Cem. Concr. Res.* **2013**, *47*, 8–13. [CrossRef]
47. Sawyer, C.N.; McCarty, P.L.; Parkin, G.F. *Chemistry for Environmental Enginnering and Science*; McGraw Hill: New York, NY, USA, 2003.
48. Dopson, M.; Johnson, D.B. Biodiversity, Metabolism and Applications of Acidophilic Sulfur-Metabolizing Microorganisms. *Environ. Microbiol.* **2012**, *14*, 2620–2631. [CrossRef]
49. Madigan, M.; Martinko, J.M.; Parker, J. *Brock Biology of Microorganisms*; Prentice-Hall: Upper Saddle River, NJ, USA, 2000.
50. Mehta, P.; Monteiro, P.J.M. *Concrete: Microstructure, Properties, and Materials*; McGraw-Hill: New York, NY, USA, 2006.

51. O'Connell, M.; McNally, C.; Richardson, M.G. Biochemical Attack on Concrete in Wastewater Applications: A State of the Art Review. *Cem. Concr. Compos.* **2010**, *32*, 479–485. [CrossRef]
52. Nnadi, E.O.; Lizarazo-Marriaga, J. Acid Corrosion of Plain and Reinforced Concrete Sewage Systems. *J. Mater. Civ. Eng.* **2013**, *25*, 1353–1356. [CrossRef]
53. Sand, W. Importance of Hydrogen Sulfide, Thiosulfate, and Methylmercaptan for Growth of Thiobacilli during Simulation of Concrete Corrosion. *Appl. Environ. Microbiol.* **1987**, *53*, 1645–1648. [CrossRef] [PubMed]
54. Islander, R.L.; Devinny, J.S.; Mansfeld, F.; Adam, P.; Hong, S. Microbial Ecology of Crown Corrosion in Sewers. *J. Environ. Eng.* **1991**, *117*, 751–770. [CrossRef]
55. Hernandez, M.; Marchand, E.A.; Roberts, D.; Peccia, J. In Situ Assessment of Active Thiobacillus Species in Corroding Concrete Sewers Using Fluorescent RNA Probes. *Int. Biodeterior. Biodegrad.* **2002**, *49*, 271–276. [CrossRef]
56. Giannantonio, D.J.; Kurth, J.C.; Kurtis, K.E.; Sobecky, P.A. Molecular Characterizations of Microbial Communities Fouling Painted and Unpainted Concrete Structures. *Int. Biodeterior. Biodegrad.* **2009**, *63*, 30–40. [CrossRef]
57. Coleman, R.N.; Gaudet, I.D. Thiobacillus Neopolitanus Implicated in the Degradation of Concrete Tanks Used for Potable Water Storage. *Water Res.* **1993**, *27*, 413–418. [CrossRef]
58. Kumar, R.; Gardoni, P.; Sanchez-Silva, M. Effect of Cumulative Seismic Damage and Corrosion on the Life-Cycle Cost of Reinforced Concrete Bridges. *Earthq. Eng. Struct. Dyn.* **2009**, *38*, 887–905. [CrossRef]
59. Yang, W.; Baji, H.; Li, C.-Q. A Theoretical Framework for Risk–Cost-Optimized Maintenance Strategy for Structures. *Int. J. Civ. Eng.* **2020**, *18*, 261–278. [CrossRef]
60. Beddoe, R.E.; Dorner, H.W. Modelling Acid Attack on Concrete: Part I. The Essential Mechanisms. *Cem. Concr. Res.* **2005**, *35*, 2333–2339. [CrossRef]
61. Ba, M.; Qian, C.; Guo, X.; Han, X. Effects of Steam Curing on Strength and Porous Structure of Concrete with Low Water/Binder Ratio. *Constr. Build. Mater.* **2011**, *25*, 123–128. [CrossRef]
62. Chen, X.; Wu, S.; Zhou, J. Influence of Porosity on Compressive and Tensile Strength of Cement Mortar. *Constr. Build. Mater.* **2013**, *40*, 869–874. [CrossRef]
63. Chindaprasirt, P.; Rukzon, S. Strength, Porosity and Corrosion Resistance of Ternary Blend Portland Cement, Rice Husk Ash and Fly Ash Mortar. *Constr. Build. Mater.* **2008**, *22*, 1601–1606. [CrossRef]
64. Kumar, R.; Bhattacharjee, B. Porosity, Pore Size Distribution and in Situ Strength of Concrete. *Cem. Concr. Res.* **2003**, *33*, 155–164. [CrossRef]
65. Mahmoodian, M.; Alani, A.M. Multi-Failure Mode Assessment of Buried Concrete Pipes Subjected to Time-Dependent Deterioration, Using System Reliability Analysis. *J Fail. Anal. Prevent.* **2013**, *13*, 634–642. [CrossRef]
66. Li, X.; Moore, L.O.; Song, Y.; Bond, P.L.; Yuan, Z.; Wilkie, S.; Hanzic, L.; Jiang, G. The Rapid Chemically Induced Corrosion of Concrete Sewers at High H 2 S Concentration. *Water Res.* **2019**, *162*, 95–104. [CrossRef]
67. De Belie, N. Microorganisms versus Stony Materials: A Love–Hate Relationship. *Mater. Struct.* **2010**, *43*, 1191–1202. [CrossRef]
68. Bohm, M.; Devinny, J.S. A Moving Boundary Diffusion Model for the Corrosion of Concrete Wastewater Systems: Simulation and Experimental Validation. In Proceedings of the 1999 American Control Conference, Cat. No. 99CH36251, San Diego, CA, USA, 2–4 June 1999; pp. 1739–1743.
69. Gutiérrez-Padilla, M.G.D.; Bielefeldt, A.; Ovtchinnikov, S.; Hernandez, M.; Silverstein, J. Biogenic Sulfuric Acid Attack on Different Types of Commercially Produced Concrete Sewer Pipes. *Cem. Concr. Res.* **2010**, *40*, 293–301. [CrossRef]
70. Ehrich, B.S.; Helard, L.; Letourneux, R.; Willocq, J.; Bock, E. Biogenic and Chemical Sulfuric Acid Corrosion of Mortars. *J. Mater. Civ. Eng.* **1999**, *11*, 340–344. [CrossRef]
71. Li, X.; Khademi, F.; Liu, Y.; Akbari, M.; Wang, C.; Bond, P.L.; Keller, J.; Jiang, G. Evaluation of Data-Driven Models for Predicting the Service Life of Concrete Sewer Pipes Subjected to Corrosion. *J. Environ. Manag.* **2019**, *234*, 431–439. [CrossRef]
72. Choi, Y.; Nesic, S.; Ling, S. Effect of H2S on the CO2 Corrosion of Carbon Steel in Acidic Solutions. *Electrochim. Acta* **2011**, *56*, 1752–1760. [CrossRef]
73. Adebayo, A.; Oluwadare, B. Corrosion of Steels in Water and Hydrogen Sulfide. *Rev. Ind. Eng. Lett.* **2014**, *1*, 80–88. [CrossRef]
74. Gharib, F.E.; Abdulhaq, A.; Abd, A. Experimental Study Of Reinforcing Steel Bars Behaviour Under Corrosive Conditions. *Aust. J. Basic Appl. Sci.* **2012**, *6*, 371–377.
75. New York State Department of Transportation. Geotechnical Aspects of Pipe Design and Installation. In *Geotechnical Design Manual*; New York State Department of Transportation: Albany, NY, USA, 2013; pp. 1–54.
76. Goodson, M.W.; Anderson, J.E. Soil-Structure Interaction–A Case Study. In Proceedings of the Structures Congress 2005, ASCE, New York, NY, USA, 20–24 April 2005; pp. 1–11.
77. ACPA. *Concrete Pipe Design Manual*; ACPA: St. Louis, MI, USA, 2011; pp. 1–540.
78. Callaghan, F.W. Pipe Performance and Experiences during Seismic Events in New Zealand over the Last 25 Years. In Proceedings of the Pipelines 2012: Innovations in Design, Construction, Operations, and Maintenance, ASCE, Miami Beach, FL, USA, 19–22 August 2012; pp. 1136–1146.
79. Rubeiz, C.G. Performance of Pipes during Earthquakes. In Proceedings of the Pipelines 2009: Infrastructure's Hidden Assets, ASCE, Miami, FL, USA, 19–22 August 2009; pp. 1205–1215.
80. Doyle, J.M.; Fang, S.J. Design of Buried Pipes. In *Handbook of Structural Engineering*; Chen, W.F., Ed.; CRC Press: Boca Raton, FL, USA, 1997; Chapter 25; ISBN 0849315697.

81. CMA. *Concrete Pipe and Portal Culvert Handbook*; CMA: Bartlett Boksburg, UK, 2012; p. 50.
82. AASHTO. *AASHTO LRFD Bridge Desig Specifications*; AASHTO: Washington, DC, USA, 2012.
83. Chughtai, F.; Zayed, T. Infrastructure Condition Prediction Models for Sustainable Sewer Pipelines. *J. Perform. Constr. Facil.* **2008**, *22*, 333–341. [CrossRef]
84. Chisala, B.N.; Lerner, D.N. Distribution of Sewer Exfiltration to Urban Groundwater. *Proc. ICE—Water Manag.* **2008**, *161*, 333–341. [CrossRef]
85. Park, S.; Lim, H.; Tamang, B.; Jin, J.; Lee, S.; Park, S.; Kim, Y.; Kim, Y. A Preliminary Study on Leakage Detection of Deteriorated Underground Sewer Pipes Using Aerial Thermal Imaging. *Int. J. Civ. Eng.* **2020**, *18*, 1167–1178. [CrossRef]
86. Scheperboer, I.C.; Luimes, R.A.; Suiker, A.S.J.; Bosco, E.; Clemens, F.H.L.R. Experimental-numerical study on the structural failure of concrete sewer pipes. *Tunn. Undergr. Sp. Technol.* **2021**, *116*, 104075. [CrossRef]
87. McCormac, J.C.; Nelson, J.K. *Design of Reinforced Concrete*; John Wiley & Sons: Hoboken, NJ, USA, 2009.
88. Products, I.; Division, E.S. *Concrete Pipe and Portal Culvert Handbook*; CMA: Bartlett Boksburg, UK, 2009.
89. CSI. *CSi Analysis Reference Manual*; Computers & Structures Inc: Walnut Creek, CA, USA, 2013.
90. González, H.D.; Reyes, G.Á. *Análisis Comparativo de La Teoría de Martson para Tuberías Enterradas y La Modelación Numérica Con Elementos Finitos*; Universidad Nacional de Colombia: Bogota, Columbia, 1999; pp. 1–13.
91. Agrawal, A.K.; Ramalingam, K.; Rozelman, S.; Kulcsar, F.; Farooqui, N. Asset Management and Nondestructive Evaluation of Force Mains in New York City. In Proceedings of the Pipelines Congress 2008, ASCE, Atlanta, GA, USA, 22–27 July 2008; pp. 1–11.
92. Ates, S. Numerical Modelling of Continuous Concrete Box Girder Bridges Considering Construction Stages. *Appl. Math. Model.* **2011**, *35*, 3809–3820. [CrossRef]
93. Bento, R.; Falcão-Silva, M.J. Analytical Model for the Seismic Behavior of Buried Pipeline when Subjected to Ground Liquefaction. In Proceedings of the 13th World Conference on Earthquake Engineering, Vancouver, BC, Canada, 1–6 August 2004.
94. Becker, G.; Boduroglu, H.; Camarinopoulos, S.; Frondistou-Yannas, S.; Gedikli, A.; Kallidromitis, V.G.; Kampranis, D.; Sanna, C. Structural Assessment and Upgrading of Sewers Based on Inspection Results. *J. Infrastruct. Syst.* **2009**, *15*, 321–329. [CrossRef]
95. Petry, T.M.; Little, D.N. Review of Stabilization of Clays and Expansive Soils in Pavements and Lightly Loaded Structures—History, Practice, and Future. *Mater. Civ. Eng.* **2002**, *16*, 447–460. [CrossRef]
96. Sert, S.; Kılıc, A.N. Numerical Investigation of Different Superstructure Loading Type Effects in Mat Foundations. *Int. J. Civ. Eng.* **2016**, *14*, 171–180. [CrossRef]
97. *ASTM C76M-14*; Standard Specification for Reinforced Concrete Culvert, Storm Drain, and Sewer Pipe (Metric). ASTM: West Conshohocken, PE, USA, 2014; pp. 1–11.
98. Sanchez-Silva, M. *Introducción a La Confiabilidad y Evaluación de Riesgos. Teoría y Aplicaciones en Ingeniería*; Universidad de los Andes, Ed.; Ediciones Uniandes: Bogota, Columbia, 2010; ISBN 9789586955119.
99. Gilman, M.J. A brief survey of stopping rules in Monte Carlo simulations. *J. Optim. Theory Appl.* **1989**, 4–9. [CrossRef]
100. Che, J.; Wang, J.; Li, K. A Monte Carlo Based Robustness Optimization Method in New Product Design Process: A Case Study. *Am. J. Ind. Bus. Manag.* **2014**, *4*, 360–369. [CrossRef]
101. *ASTM C1417 M*; Standard Specification for Manufacture of Reinforced Concrete Sewer, Storm Drain, and Culvert Pipe for Direct Design [Metric]. ASTM: West Conshohocken, PE, USA, 2014; pp. 1–7.
102. *ASTM C1433 M*; Standard Specification for Precast Reinforced Concrete Monolithic Box Sections for Culverts, Storm Drains and Sewers. ASTM: West Conshohocken, PE, USA, 2014; pp. 1–22.
103. *ASTM C655M-14*; Standard Specification for Reinforced Concrete D-Load Culvert, Storm Drain, and Sewer Pipe (Metric). ASTM: West Conshohocken, PE, USA, 2014; pp. 1–6.
104. del Giudice, G.; Padulano, R.; Siciliano, D. Multivariate probability distribution for sewer system vulnerability assessment under data-limited conditions. *Water Sci. Technol.* **2016**, *73*, 751–760. [CrossRef] [PubMed]
105. Dirksen, J.; Clemens, L.R. Probabilistic modeling of sewer deterioration using inspection data inspection data. *Water Sci. Technol.* **2008**, *57*, 1635–1641. [CrossRef] [PubMed]
106. Laakso, T.; Kokkonen, T.; Mellin, I.; Vahala, R. Sewer Life Span Prediction: Comparison of Methods and Assessment of the Sample Impact on the Results. *Water* **2019**, *11*, 2657. [CrossRef]
107. Caradot, N. *The Use of Deterioration Modelling to Simulate Sewer Asset Management Strategies*; INSA Université de Lyon: Lyon, France, 2019.
108. Hernández, N.R. *Methodology for Identifying the Key and Enough Factors for Achieving Objectives in Sewer Asset Management*; Pontificia Universidad Javeriana: Bogota, Columbia, 2020.
109. Fugledalen, T.; Rokstad, M.M.; Tscheikner-Gratl, F. On the influence of input data uncertainty on sewer deterioration models—A case study. *Struct. Infrastruct. Eng.* **2021**, 1–12. [CrossRef]
110. Jin, Y.; Mukherjee, A.; Asce, A.M. Modeling Blockage Failures in Sewer Systems to Support Maintenance Decision Making. *J. Perform. Constr. Facil.* **2010**, *24*, 622–633. [CrossRef]
111. Korving, H.; van Noortwijk, J.M.; van Gelder, P.H.A.J.M.; Clemens, H.L.R.; Korving, H.; van Noortwijk, J.M.; van Gelder, P.H.A.J.M. Risk-based design of sewer system rehabilitation. *Struct. Infrastruct. Eng.* **2009**, *5*, 215–227. [CrossRef]
112. ACPA. *Highway Live Loads on Concrete Pipe*; ACPA: St. Louis, MI, USA, 2009; Volume 1, pp. 1–10.
113. Zamanian, S.; Hur, J.; Shafieezadeh, A. Significant variables for leakage and collapse of buried concrete sewer pipes: A global sensitivity analysis via Bayesian additive regression trees and Sobol' indices. *Struct. Infrastruct. Eng.* **2021**, *17*, 676–688. [CrossRef]

114. Qiu, L.; Dong, S.; Ashour, A.; Han, B. Antimicrobial concrete for smart and durable infrastructures: A review. *Constr. Build. Mater.* **2020**, *260*, 1–15. [CrossRef]
115. Jamshidi, M.; Alizadeh, M.; Salar, M.; Hashemi, A. Durability of Polyester Resin Concrete in Different Chemical Solutions. *Adv. Mater. Res.* **2013**, *687*, 150–154. [CrossRef]
116. Meyer-Policrete. *POLYCRETE Catalog*; Meyer: Stendal: Germany, 2020; pp. 1–16.
117. Resin, N.P.G.P.; Relining, P. *CRYSTIC PD10098T. Ortho—NPG Polyester Resin for Pipe Relining*; Scott Bader SAS: Amiens, France, 2018; pp. 1–2.
118. TPP Manufacturing. Polyester resin concrete jacking pipe. In *Product Type Specification*; TPP Manufacturing: Singapore, 2016; pp. 1–2.
119. *DIN 16946-2*; Cured Casting Resins: Types. German Institute for Standardisation (DIN): Berlin, Germany, 1989; 8p.